

## Investigation on the effect of natural kaolin substitution on geopolymer mortar made by a combination of fly ash and rice husk ash

Arie Wardhono<sup>1\*</sup>,  Mochamad Firmansyah Sofianto<sup>2</sup>,  Meity Wulandari<sup>3</sup>

<sup>1,2,3</sup>Department of Civil Engineering, Universitas Negeri Surabaya, Surabaya 60231, Indonesia; ariewardhono@unesa.ac.id (A.W.) mochamadfirmansyah@unesa.ac.id (M.F.S.) meitywulandari@unesa.ac.id (M.W.).

**Abstract:** This study aims to investigate the potential of using natural kaolin (NKL) as a substitute for rice husk ash (RHA) in fly ash-rice husk ash-based geopolymer mortar (FARH-GM) applications as eco-friendly materials. The effect of NKL substitution was investigated by compressive strength, porosity, and depth penetration tests at 1%, 2%, and 3% of the composition in FARH-GM. The chemical compound analysis was identified using XRF and XRD techniques. The results showed that the 2% NKL substitution for RHA demonstrates the highest compressive strength and the lowest porosity value of FARH-GM, with a final setting time of 3.5 hours. However, increasing the NKL substitution ratio by more than 2% significantly decreases the strength performance and tends to prolong the setting time. The substitution of NKL also considerably affects the Si/Al and Si/Fe ratios, which increase along with the increase of NKL. The highest strength was achieved with Si/Al and Si/Fe ratios of 4.59 and 1.71, respectively. Furthermore, higher NKL substitution tends to increase the crystalline peak, indicating the presence of albite, anorthite, and cristobalite crystalline phases. These results suggest that natural kaolin can be used as a substitute in geopolymer applications at a specific ratio.

**Keywords:** Fly Ash, Geopolymer, Mortar, Natural Kaolin Substitution, Rice Husk Ash.

### 1. Introduction

The innovation of geopolymer as an environmentally friendly material to replace the role of Portland Cement (PC) has demonstrated quite significant development. As the primary material in concrete production, the PC production process is one of the largest producers of CO<sub>2</sub> gas, which triggers global climate change [1-3]. This encourages the search for environmentally friendly alternative materials. One alternative to address this issue is using fly ash (FA) and rice husk ash (RHA) as environmentally friendly waste materials.

FA, a waste material from the coal combustion process in power plants, can be used as a PC replacement alternative material [4-7]. The primary composition of fly ash is silicate (Si), aluminate (Al), and ferrite (Fe) with reasonably low calcium (Ca) content [5, 6]. Recent studies have shown that concrete can be produced using FA reacted with an alkaline activator [8-11]. This material is known as geopolymer [12]. PC-based concrete binders are formed from the reaction between Ca and Si, which forms a calcium-silicate-hydrate (C-S-H) gel. The mechanism of the geopolymer matrix is the reaction between Si and Al, which forms an inorganic binder through a polymer reaction, forming an N-A-S-H matrix [13, 14].

In recent studies, the use of FA as the primary material of geopolymers can be combined with RHA, a waste material from burning rice husks [15, 16]. This is due to the characteristics of the chemical composition of RHA, which are dominated by the Si component, which can fill the role of Si in the N-A-S-H geopolymer matrix, especially in the -Si-O-Al-O- bond in the N-A-S-H geopolymer chain [17, 18]. In addition, RHA has pozzolanic properties that can improve geopolymer performance [19]. According

to Hossain, et al. [20] the incorporation of 10wt% of RHA improved geopolymer's short- and long-term properties. Hwang and Huynh [21] found that RHA content of 35% in geopolymer exhibited the highest compressive strength. However, treatment for the RHA is required to alter its compound. In addition, Ogwang, et al. [22] used 30% of RHA in developing a metakaolin-RHA-based geopolymer. The RHA was generated by firing the rice husks at 600°C to achieve an amorphous phase. Based on this, it can be determined that the maximum use of un-treatment RHA in geopolymer can only be achieved at 10%. RHA waste also supports the concept of a green economy and eco-friendly materials.

However, the main issue with the combination of FA and RHA is the low Al content, which plays an important role in the -Si-O-Al-O- matrix. This impacts the geopolymer strength, which cannot achieve the required strength. Based on previous research, the geopolymer manufacturing process requires sufficient Si and Al composition for the N-A-S-H geopolymer matrix [14, 23]. The addition of RHA can indeed increase the strength of geopolymer materials through -Si-O-Al-O- bonds. However, the high content of unreacted Si due to the low Al content tends to reduce the strength performance of geopolymer materials [24]. Thus, it is necessary to find materials with Si and Al contents. One alternative is to use natural kaolin (NKL), a white clay material that is widely used in the ceramics and paper industries [25]. The primary chemical composition of NKL is Si and Al [26]. Most research reports use NKL as a substitution in FA or NKL in NKL-based geopolymer. While other recent studies are focused on altering NKL properties or using meta-kaolin (MKL) in geopolymer [26-31]. Research on using NKL as a substitute for FA and RHA-based geopolymers (FARH-GM) is still very limited. It aims to reduce energy consumption and the cost of altering NKL properties. This study researches the potential of using NKL as a substitution for RHA at the rate of 1%, 2%, and 3% of the composition in FARH-GM. The effect of NKL substitution was investigated by compressive strength and porosity tests. These results were supported by setting time tests, XRF, and XRD analyses to provide a deep understanding of the NKL substitution. This study is expected to optimize the use of environmentally friendly waste materials that have the potential to address global warming issues.

## 2. Experimental Methods

### 2.1. Materials

The primary materials of geopolymer mortar were FA and RHA, while NKL was used as a substitution for RHA. FA was obtained from coal power plants, while RHA was produced from the remains of burning rice husks locally from paddylands. FA was categorized as class C FA with a total amount of  $\text{SiO}_2 + \text{Al}_2\text{O}_3 + \text{Fe}_2\text{O}_3$  of 69.6% and CaO content of 21.9%, conforming to ASTM C618 [32]. The specific gravity of FA, RHA, and NKL were 2.43, 1.25, and 2.12, respectively. All materials were supplied and commercially available in Indonesia. Table 1 gives the chemical compositions of all materials. The materials were identified by X-ray fluorescence (XRF) test using PANalytical type Minipal four equipment.

**Table 1.**  
Chemical composition of materials (%)

| Compound | SiO <sub>2</sub> | Al <sub>2</sub> O <sub>3</sub> | Fe <sub>2</sub> O <sub>3</sub> | CaO  | K <sub>2</sub> O | MnO  | TiO <sub>2</sub> |
|----------|------------------|--------------------------------|--------------------------------|------|------------------|------|------------------|
| FA       | 30.4             | 11.8                           | 27.4                           | 21.9 | 2.14             | 0.22 | 1.43             |
| RHA      | 92.7             | -                              | 0.32                           | 1.57 | -                | 0.26 | 0.03             |
| NKL      | 57.6             | 37.1                           | 2.79                           | 0.32 | 1.58             | 0.04 | 0.66             |

Note: FA = Fly ash, RHA = Rice husk ash, NKL = Natural kaolin.

The X-ray diffraction pattern of all materials was performed using an XRD test using PANalytical type X'Pert PRO equipment, as shown in Figure 1. The XRD analysis of FA showed an amorphous phase (indicated by the broad hump at approximately 15° to 36° 2-theta) with crystalline peaks characterized as quartz and magnetite. The RHA diffraction pattern exhibited an amorphous of silica particles observed by the broadening of the peak at approximately 18° to 22° 2-theta. At the same time, the NKL diffraction pattern displayed a crystalline pattern dominated by kaolinite.

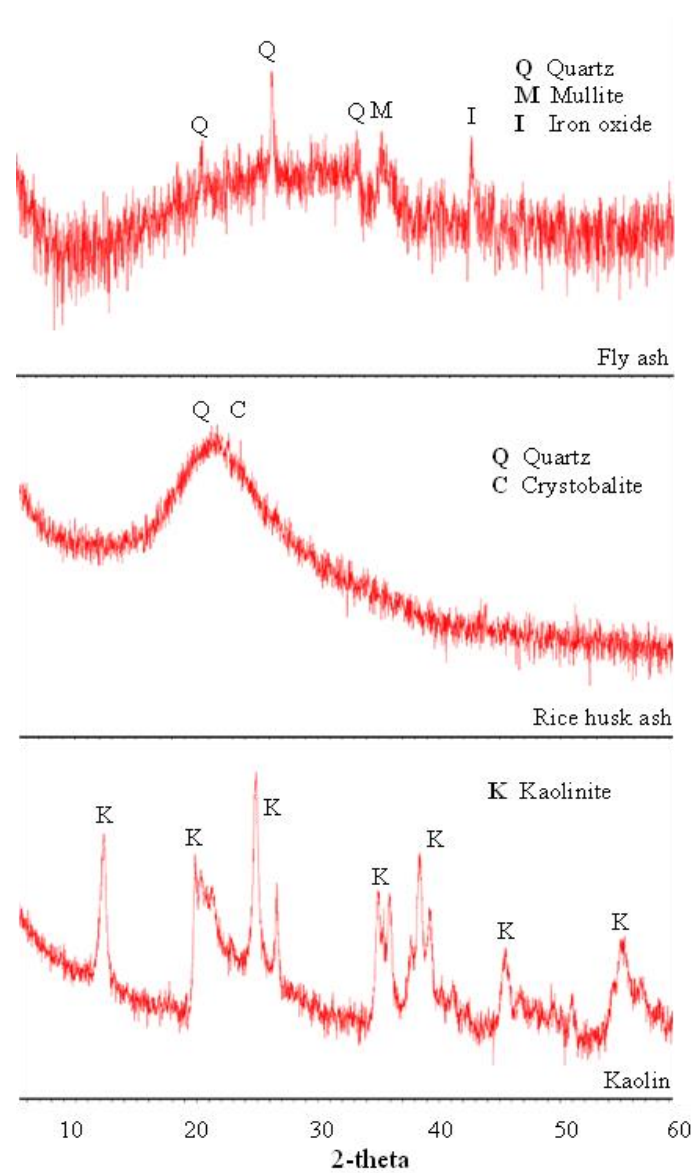


**Figure 1.**  
XRD pattern of fly as, rice husk ash, and kaolin

## 2.2. Mix Compositions

The FARH-GM mix composition is displayed in Table 2. Initial research determined that FA and RHA were the primary materials forming geopolymer mortar with a composition of 90% FA and 10% RHA (Control). The use of NKL was determined at 1%, 2%, and 3% of the composition of RHA in geopolymer mix compositions to assess the influence of NKL as a partial substitute for RHA. It designated as 1% NKL, 2% NKL, and 3% NKL for 1%, 2%, and 3% natural kaolin substitution, respectively. The ratio of total FA, RHA, and NKL to fine aggregate was kept at 1:2.75, conforming to ASTM C109 [33].

A combination of sodium silicate ( $\text{Na}_2\text{SiO}_3$ ) and sodium hydroxide ( $\text{NaOH}$ ) 8 Molar was used as an alkali activator solution. The liquid sodium silicate had  $\text{Na}_2\text{O}$  and  $\text{Na}_2\text{SiO}_3$  contents of 9.2% and 30.5%, respectively. The 8-molar  $\text{NaOH}$  solution was prepared by dissolving 320 grams of  $\text{NaOH}$  pellets in 1

liter of distilled water. The sodium silicate to NaOH ratio was kept at 2.0. The fine aggregate was natural sand with a specific gravity of 2.61 and a fineness modulus 2.02. All materials were provided by a local supplier in Surabaya, Indonesia

**Table 2.**

Mix composition of geopolymer mortar (kg/m<sup>3</sup>)

| Mix design | NKL substitution | FA  | RHA | NKL | FAGR | SS  | NaOH 8M | Water |
|------------|------------------|-----|-----|-----|------|-----|---------|-------|
| Control    | 0%               | 500 | -   | -   | 1373 | 172 | 85      | 76    |
| 1% NKL     | 1%               | 450 | 45  | 5   | 1373 | 172 | 85      | 76    |
| 2% NKL     | 2%               | 450 | 40  | 10  | 1373 | 172 | 85      | 76    |
| 3% NKL     | 3%               | 450 | 35  | 15  | 1373 | 172 | 85      | 76    |

**Note:** FAGR = Fine aggregate, SS = Sodium silicate, NaOH 8M = Sodium hydroxide 8 Molar

### 2.3. Specimen Preparation and Testing

The FARH-GM mortar specimens were prepared using 50-mm cube steel molds following ASTM C109 [33]. The specimens were kept at room temperature after casting for 24 hours. The specimens were removed from the mold and subjected to heat curing at 100°C for 24 hours. This is due to the forming process of the geopolymer matrix, which requires a high temperature to accelerate the polymerization process [34–36]. The geopolymer mortar specimens were stored at room temperature before testing.

The strength performance of geopolymer mortar specimens was carried out by compressive strength test conforming ASTM C109 [33] and porosity test following ASTM C642 [37]. The porosity test was performed to investigate the pore voids of geopolymer mortar as supporting data for the compressive strength test results. All specimens were tested at 7 and 28 days. Three mortar specimens were tested for each data point. The setting time of geopolymer specimens was investigated by depth penetration test (Vicat) conforming ASTM C191 to identify the effect of kaolin substitution on the initial and final setting time of geopolymer specimens [38]. The XRF analysis was carried out using PANalytical type Minipal four equipment to identify the alteration of chemical compounds. XRD analysis was conducted to identify and characterize the crystalline phase in fly ash-rice husk ash geopolymer specimens due to the kaolin substitution. The test was performed using PANalytical type X'Pert PRO equipment.

## 3. Results and Discussions

### 3.1. Compressive Strength and Porosity

The results of NKL substitution on compressive strength and porosity development of FARH-GM are given in Figure 2–3. In Figure 2, it is clearly seen that NKL substitution on RHA significantly affected the strength development of FARH-GM at 7 and 28 days. All geopolymer specimens also exhibited a significant increase in strength from 7 to 28 days. A significant increase was observed from 0% NKL ( $21.7 \pm 1.1$  MPa) to 1% NKL ( $32.2 \pm 1.9$  MPa) substitution. The highest compressive was achieved by 2% NKL ( $34.7 \pm 1.7$  MPa) substitution at 28 days. It might be attributed to the addition of Al content from NKL, which reacts with Si to form a -Si-O-Al-O- geopolymer matrix and increases the compressive strength [39, 40]. This result was corroborated by the porosity test results, as shown in Figure 3. The substitution of NKL for RHA increased the density of FARH-GM. This can be seen in the decrease in pores value at the substitution of 1% NKL. The 1%-2% NKL substitution demonstrated denser pores compared to other specimens.

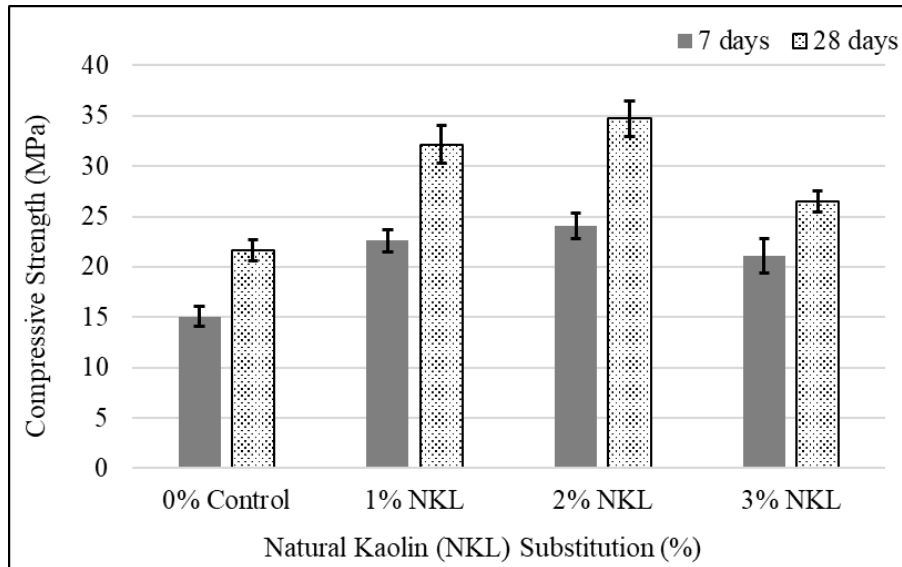


**Figure 2.**  
The effect of NKL substitution on compressive strength development

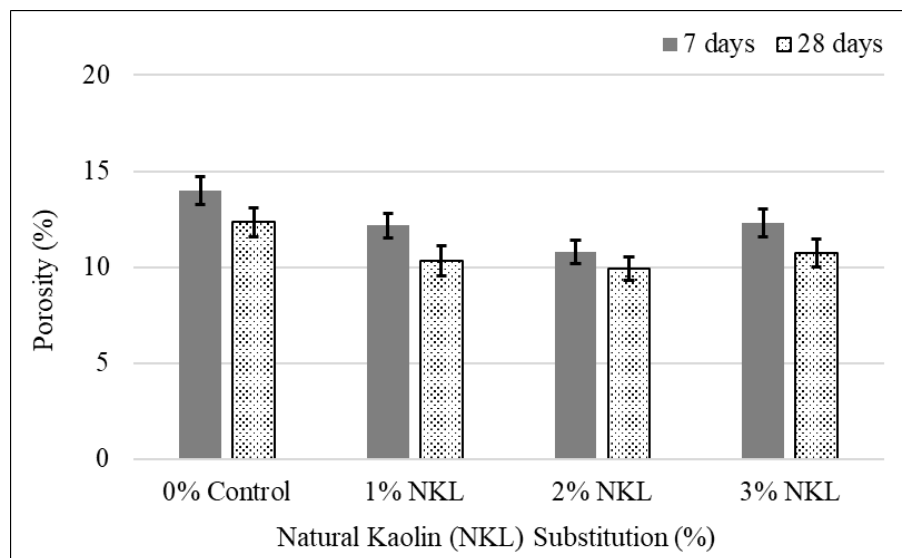


**Figure 3.**  
The effect of NKL substitution on porosity

In this study, it should be noted that there was merely a slight performance improvement in 1%-2% NKL substitution. In terms of strength development, it was observed that there was no significant increase from 1% to 2% NKL substitution. The standard deviation indicated that it might exhibit a similar strength performance between 1% and 2% NKL substitution. The porosity value was also performed similar trends. This might indicate that the Si and Al contents have achieved their balanced or a specific silicate-to-aluminate ratio to form the -Si-O-Al-O- matrix bonds. However, the use of NKL of more than 2% tends to reduce the performance of FARH-GM specimens. It can be seen in a significant decrease in strength performance in 3% NKL. This is supported by the porosity value, which increases with the addition of the NKL ratio. Although the NKL addition increases the Al content in the geopolymer matrix, it further reduces the amorphous component. The XRD results on RHA and NKL

materials show that RHA has more amorphous contents than NKL. Thus, the further substitution of RHA by NKL tends to reduce the amorphous components and significantly affect the performance of the geopolymer specimens.

### 3.2. Setting Time Analysis

Figure 4 shows the results of the depth penetration test. It gives information regarding the initial and final setting time of FARH-GM specimens due to the NKL substitution. The substitution of NKL significantly affected the setting time of the geopolymer specimen. Substituting 1% NKL exhibited a faster initial and final setting time. However, increasing the NKL in geopolymer tends to prolong the setting time. The initial setting time of 1% NKL occurred at 0.5 hours, while 2% NKL and 3% NKL substitution showed a slower setting time rate, which occurred after 1 hour.

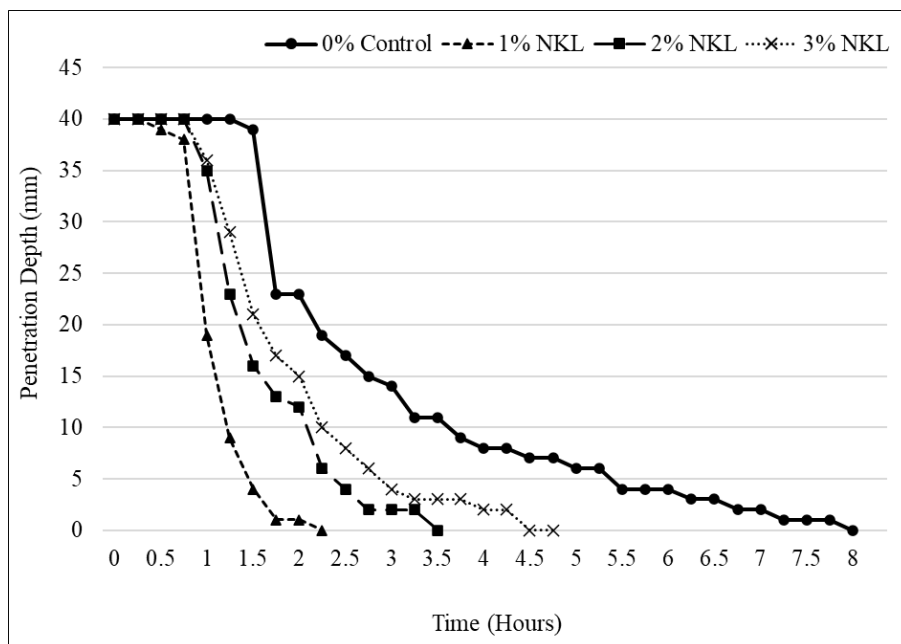


**Figure 4.**  
The effect of NKL substitution on setting time.

This study found that higher NKL substitution significantly decreased the final setting time of FARH-GM. It took a longer time to achieve reaction stability and structural integrity. The final setting time of 1% NKL was completed in 2.5 hours. While, 2% NKL and 3% NKL only reached the final setting time in 3.5 and 4.5 hours, respectively. This could be attributed to the amorphous compounds and CaO contents in geopolymer. The higher NKL ratio substitution in geopolymer decreased the amorphous and CaO compounds, which prolonged the geopolymer reaction rate. According to Deb, et al. [41]. The use of high Ca-content material significantly affects the setting and strength of the development of geopolymers.

### 3.3. Chemical Composition Analysis

The chemical composition of FARH-GM with NKL substitution was analyzed using XRF and XRD techniques. The XRF analysis presents the chemical compound of FARH-GM with 1%, 2%, and 3% NKL substitution in Table 3. It consisted of the primary material for the geopolymer, i.e., SiO<sub>2</sub>, Al<sub>2</sub>O<sub>3</sub>, Fe<sub>2</sub>O<sub>3</sub>, and other compounds such as CaO, K<sub>2</sub>O, MnO, and TiO<sub>2</sub>. As predicted, this corresponds to the geopolymer primary matrix components comprising N-A-S-H [9, 14]. The XRF analysis showed that

the  $\text{SiO}_2$  compound increased along with the NKL substitution. While the  $\text{Al}_2\text{O}_3$  and  $\text{Fe}_2\text{O}_3$  tend to decrease. The increase in the  $\text{SiO}_2$  compound was due to the high Si content in RHA and NKL materials. The decrease of  $\text{Al}_2\text{O}_3$  and  $\text{Fe}_2\text{O}_3$  might attributed to the geopolymeric reaction between Si, Al, and Fe, forming a geopolymer matrix of polysialates and ferrosialates [42-44].

**Table 3.**

Chemical composition of fly ash-rice husk ash-based geopolymer with kaolin substitution (%)

| Mix design | $\text{SiO}_2$ | $\text{Al}_2\text{O}_3$ | $\text{Fe}_2\text{O}_3$ | $\text{CaO}$ | $\text{K}_2\text{O}$ | $\text{MnO}$ | $\text{TiO}_2$ |
|------------|----------------|-------------------------|-------------------------|--------------|----------------------|--------------|----------------|
| Control    | 35.7           | 9.9                     | 28.1                    | 19.9         | 1.87                 | 0.34         | 1.69           |
| 1% NKL     | 40.7           | 9.6                     | 25.6                    | 17.8         | 2.01                 | 0.33         | 1.46           |
| 2% NKL     | 41.8           | 9.1                     | 24.5                    | 17.2         | 2.03                 | 0.31         | 1.39           |
| 3% NKL     | 46.6           | 8.5                     | 23.1                    | 16.1         | 2.04                 | 0.31         | 1.35           |

Figure 5 exhibits the  $\text{SiO}_2/\text{Al}_2\text{O}_3$  and  $\text{SiO}_2/\text{Fe}_2\text{O}_3$  ratio change due to NKL inclusion. It found that the  $\text{SiO}_2/\text{Al}_2\text{O}_3$  ratio increased along with the NKL addition. It correlated with the incorporation of Al into the structure of the geopolymer matrix. The high performance of FARH-GM was achieved at a  $\text{SiO}_2/\text{Al}_2\text{O}_3$  ratio of 4.59 (2% NKL). However, increasing the NKL ratio by more than 2% tends to decrease the strength performance. It might be attributed to the worse chemical stability at a higher  $\text{SiO}_2/\text{Al}_2\text{O}_3$  ratio [39]. In addition, Wang, et al. [40] stated that the mechanical properties of geopolymer tend to decrease at a high  $\text{SiO}_2/\text{Al}_2\text{O}_3$  ratio due to the instability of the molecular structure of the geopolymer matrix. Similar to the  $\text{SiO}_2/\text{Al}_2\text{O}_3$  ratio, the ratio of  $\text{SiO}_2/\text{Fe}_2\text{O}_3$  also increased at higher NKL substitution. It exhibited the inclusion of  $\text{Fe}^{2+}$  ions in the geopolymer matrix [44].

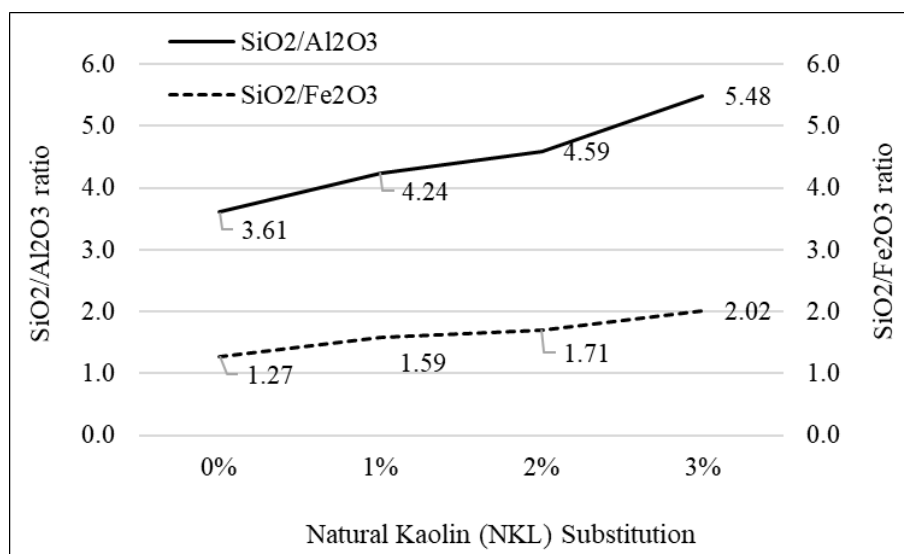


**Figure 5.**  
The effect of NKL substitution on  $\text{SiO}_2/\text{Al}_2\text{O}_3$  ratio and CaO content

Figure 6 shows the XRD pattern of FARH-GM with NKL substitution. All specimens indicated the presence of crystalline phases of albite ( $\text{NaAlSi}_3\text{O}_8$ ), anorthite ( $\text{CaAl}_2\text{Si}_2\text{O}_8$ ), and cristobalite ( $\text{SiO}_2$ ). Albite and anorthite peaks were associated with the raw FA, RHA, and NKL, which have high Si and Al contents. However, the kaolinite peaks were not found in all specimens. It could be attributed to the geopolymer reaction. According to Matalkah, et al. [28] and Ramli, et al. [30] these kaolinite peaks decreased during a high sintering temperature process. Further, there was also a slight appearance of cristobalite, which might be attributed to the unreacted quartz ( $\text{SiO}_2$ ) from the raw materials.

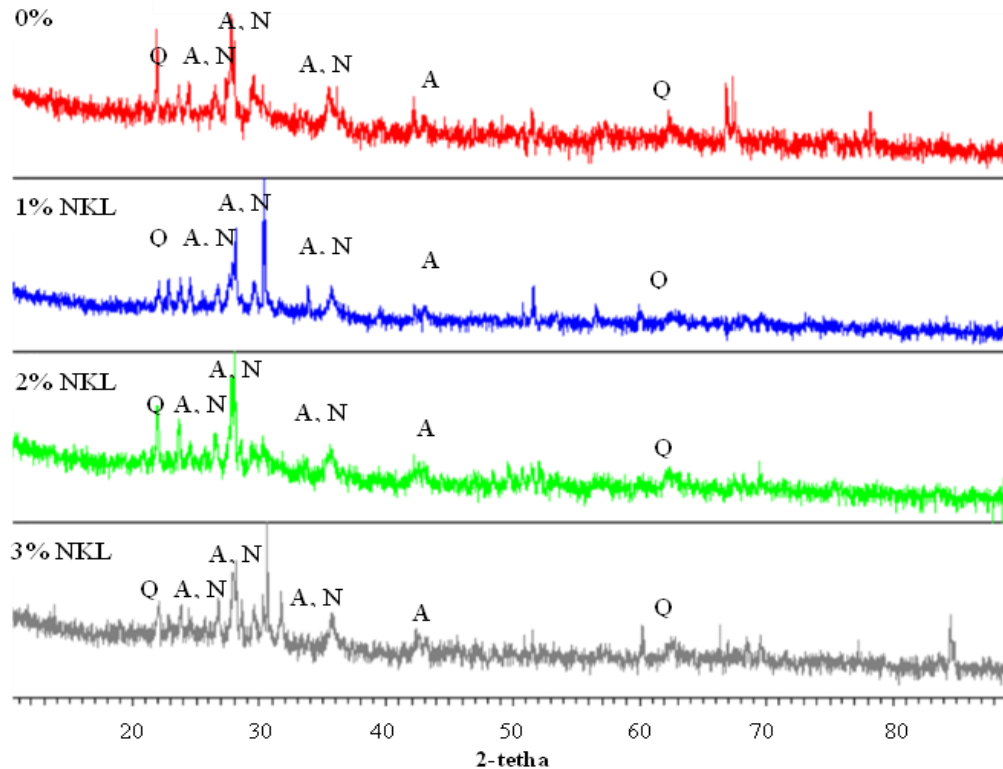


Figure 6. XRD pattern of FARH-GM with NKL substitution (A: Albite, N: Anorthite, C: Cristobalite)

In this study, it was found that the increase of crystalline peak occurred along with the increase of NKL substitution. According to Patrisia, et al. [44] this indicated that the amorphous components from raw materials were converted into crystalline components during the geopolymerization reaction in geopolymer. This confirmed the change in the crystalline phase that occurs in 1% to 3% NKL substitution, where the crystalline phase increases along with the increase in kaolin substitution.

#### 4. Conclusions

This study investigated the potential of using NKL as a substitution for RHA in a specific ratio in FARH-GM. Based on the results and discussions, the following conclusions are drawn.

1. The 2% NKL substitution to RHA demonstrates the highest performance of FARH-GM. It achieved the highest compressive strength of  $34.7 \pm 1.7$  MPa and the lowest porosity value. However, increasing the NKL substitution ratio by more than 2% significantly decreases the strength performance.
2. The substitution of NKL significantly affected the setting time of the FARH-GM. Substituting 1% NKL exhibited a faster initial and final setting time. However, increasing the NKL by more than 1% in geopolymer prolongs the setting time.
3. The substitution of NKL significantly affects the Si/Al and Si/Fe ratios. It increases along with the increase of NKL. It achieves the highest strength at 2% NKL substitution with Si/Al and Si/Fe ratios of 4.59 and 1.71, respectively. Substituting NKL more than 2% tends to decrease the strength of FARH-GM.
4. Increasing NKL substitution affects the crystalline phase of FARH-GM. Higher NKL substitution tends to increase the crystalline peak, indicating the presence of albite, anorthite, and cristobalite crystalline phases.



5. NKL can be used as a substitution for RHA in FARH-GM at a specific ratio. It also supports the use of more environmentally friendly waste materials that have the potential to address global warming issues.

### Funding:

The authors declare that this work was supported by Universitas Negeri Surabaya, Indonesia.

### Transparency:

The authors confirm that the manuscript is an honest, accurate, and transparent account of the study; that no vital features of the study have been omitted; and that any discrepancies from the study as planned have been explained. This study followed all ethical practices during writing.

### Copyright:

© 2025 by the authors. This open-access article is distributed under the terms and conditions of the Creative Commons Attribution (CC BY) license (<https://creativecommons.org/licenses/by/4.0/>).

### References

- [1] M. Schneider, "The cement industry on the way to a low-carbon future," *Cement and Concrete Research*, vol. 124, p. 105792, 2019. <https://doi.org/10.1016/j.cemconres.2019.105792>
- [2] V. Shobeiri, B. Bennett, T. Xie, and P. Visintin, "A comprehensive assessment of the global warming potential of geopolymer concrete," *Journal of Cleaner Production*, vol. 297, p. 126669, 2021. <https://doi.org/10.1016/j.jclepro.2021.126669>
- [3] S. Nie *et al.*, "Analysis of theoretical carbon dioxide emissions from cement production: Methodology and application," *Journal of Cleaner Production*, vol. 334, p. 130270, 2022. <https://doi.org/10.1016/j.jclepro.2021.130270>
- [4] A. K. Saha, "Effect of class F fly ash on the durability properties of concrete," *Sustainable Environment Research*, vol. 28, no. 1, pp. 25-31, 2018. <https://doi.org/10.1016/j.serj.2017.09.001>
- [5] S. S. Alterary and N. H. Marei, "Fly ash properties, characterization, and applications: A review," *Journal of King Saud University-Science*, vol. 33, no. 6, p. 101536, 2021. <https://doi.org/10.1016/j.jksus.2021.101536>
- [6] D. K. Nayak, P. Abhilash, R. Singh, R. Kumar, and V. Kumar, "Fly ash for sustainable construction: A review of fly ash concrete and its beneficial use case studies," *Cleaner Materials*, vol. 6, p. 100143, 2022. <https://doi.org/10.1016/j.clema.2022.100143>
- [7] A. Wardhono *et al.*, "The ratio of alkali modulus in strength development of class c fly ash geopolymer mortar," presented at the 3rd International Conference of Green Civil and Environmental Engineering, 2021.
- [8] X. Y. Zhuang *et al.*, "Fly ash-based geopolymer: Clean production, properties and applications," *Journal of Cleaner Production*, vol. 125, pp. 253-267, 2016. <https://doi.org/10.1016/j.jclepro.2016.03.019>
- [9] A. Wardhono, "The effect of sodium hydroxide molarity on strength development of non-cement class c fly ash geopolymer mortar," *Journal of Physics: Conference Series*, vol. 288, no. 1, p. 012001, 2018. <https://doi.org/10.1088/1742-6596/947/1/012001>
- [10] T. Mashifana, "Geo-polymerized cementitious material as a stabilizer of waste fly ash to produce green building bricks," *Journal of Sustainable Construction Materials and Technologies*, vol. 6, no. 2, pp. 63-69, 2021. <https://doi.org/10.29187/jscmt.2021.61>
- [11] D. Law, C. Gunasekara, Y. Patrisia, S. Fernando, and A. Wardhono, "Development of durable class F fly ash based geopolymer concretes," *Sustainable Sustainable Environment and Architecture*, vol. 1157, no. 1, p. 012024, 2023. <https://doi.org/10.1088/1755-1315/1157/1/012024>
- [12] V. Živica, M. T. Palou, and M. Križma, "Geopolymer cements and their properties: A review," *Building Research Journal*, vol. 61, no. 2, pp. 85-100, 2015. <https://doi.org/10.2478/brj-2014-0007>
- [13] N. Singh, M. Kumar, and S. Rai, "Geopolymer cement and concrete: Properties," *Materials Today: Proceedings*, vol. 29, pp. 743-748, 2020. <https://doi.org/10.1016/j.matpr.2020.04.513>
- [14] N. Shehata, O. Mohamed, E. T. Sayed, M. A. Abdelkareem, and A. Olabi, "Geopolymer concrete as green building materials: Recent applications, sustainable development and circular economy potentials," *Science of the Total Environment*, vol. 836, p. 155577, 2022. <https://doi.org/10.1016/j.scitotenv.2022.155577>
- [15] S. K. Das, J. Mishra, and S. M. Mustakim, "Rice husk ash as a potential source material for geopolymer concrete: A," *International Journal of Applied Engineering Research*, vol. 13, pp. 81-84, 2018. <https://doi.org/10.37622/IJAER/13.7.2018.81-84>

- [16] A. Siddika, M. A. Al Mamun, R. Alyousef, and H. Mohammadhosseini, "State-of-the-art-review on rice husk ash: A supplementary cementitious material in concrete," *Journal of King Saud University-Engineering Sciences*, vol. 33, no. 5, pp. 294-307, 2021. <https://doi.org/10.1016/j.jksues.2020.10.006>
- [17] K. Chiranjeevi, M. Vijayalakshmi, and T. Praveenkumar, "Investigation of fly ash and rice husk ash-based geopolymer concrete using nano particles," *Applied Nanoscience*, vol. 13, no. 1, pp. 839-846, 2023. <https://doi.org/10.1007/s13204-021-01916-2>
- [18] Y. Zhao, B. Chen, and H. Duan, "Effect of rice husk ash on properties of slag based geopolymer pastes," *Journal of Building Engineering*, vol. 76, p. 107035, 2023. <https://doi.org/10.1016/j.jobbe.2023.107035>
- [19] S. A. Saad, M. F. Nuruddin, N. Shafiq, and M. Ali, "Pozzolanic reaction mechanism of rice husk ash in concrete—a review," *Applied Mechanics and Materials*, vol. 773, pp. 1143-1147, 2015. <https://doi.org/10.4028/www.scientific.net/AMM.773-774.1143>
- [20] S. S. Hossain, P. Roy, and C.-J. Bae, "Utilization of waste rice husk ash for sustainable geopolymer: A review," *Construction and Building Materials*, vol. 310, p. 125218, 2021. <https://doi.org/10.1016/j.conbuildmat.2021.125218>
- [21] C.-L. Hwang and T.-P. Huynh, "Effect of alkali-activator and rice husk ash content on strength development of fly ash and residual rice husk ash-based geopolymers," *Construction and Building Materials*, vol. 101, pp. 1-9, 2015. <https://doi.org/10.1016/j.conbuildmat.2015.10.025>
- [22] G. Ogwang, P. Olupot, H. Kasedde, E. Menya, H. Storz, and Y. Kiros, "Experimental evaluation of rice husk ash for applications in geopolymer mortars," *Journal of Bioresources and Bioproducts*, vol. 6, no. 2, pp. 160-167, 2021. <https://doi.org/10.1016/j.jobab.2021.02.008>
- [23] H. Gökçe, M. Tuyan, and M. Nehdi, "Alkali-activated and geopolymer materials developed using innovative manufacturing techniques: A critical review," *Construction and Building Materials*, vol. 303, p. 124483, 2021. <https://doi.org/10.1016/j.conbuildmat.2021.124483>
- [24] C. Tennakoon, P. De Silva, K. Sagoe-Crentsil, and J. G. Sanjayan, "Influence and role of feedstock Si and Al content in Geopolymer synthesis," *Journal of Sustainable Cement-Based Materials*, vol. 4, no. 2, pp. 129-139, 2015. <https://doi.org/10.1080/21650373.2014.979264>
- [25] H. H. Murray, "Kaolin applications," *Developments in Clay Science*, vol. 2, pp. 85-109, 2006. [https://doi.org/10.1016/S1572-4352\(06\)02005-8](https://doi.org/10.1016/S1572-4352(06)02005-8)
- [26] A. Kabirova and M. Uysal, "Influence of rice husk ash substitution on some physical, mechanical and durability properties of the metakaolin-based geopolymer mortar," *Journal of Sustainable Construction Materials and Technologies*, vol. 7, no. 2, pp. 88-94, 2022. <https://doi.org/10.47481/jscmt.1093312>
- [27] F. Okoye, J. Durgaprasad, and N. Singh, "Mechanical properties of alkali activated flyash/Kaolin based geopolymer concrete," *Construction and Building Materials*, vol. 98, pp. 685-691, 2015. <https://doi.org/10.1016/j.conbuildmat.2015.08.009>
- [28] F. Matalkah, R. Aqel, and A. Ababneh, "Enhancement of the mechanical properties of kaolin geopolymer using sodium hydroxide and calcium oxide," *Procedia Manufacturing*, vol. 44, pp. 164-171, 2020. <https://doi.org/10.1016/j.promfg.2020.02.218>
- [29] O. F. Nnaemeka and N. Singh, "Durability properties of geopolymer concrete made from fly ash in presence of Kaolin," *Materials Today: Proceedings*, vol. 29, pp. 781-784, 2020. <https://doi.org/10.1016/j.matpr.2020.04.696>
- [30] M. I. I. Ramli *et al.*, "The influence of sintering temperature on the pore structure of an alkali-activated kaolin-based geopolymer ceramic," *Materials*, vol. 15, no. 7, p. 2667, 2022. <https://doi.org/10.3390/ma15072667>
- [31] M. Kaya, S. İlkentapar, U. Durak, İ. İ. Atabey, and S. Çelikten, "Physical mechanical and microstructural properties of kaolin-based fly ash-added geopolymer mortars," *Iranian Journal of Science and Technology, Transactions of Civil Engineering*, vol. 48, no. 5, pp. 3559-3572, 2024. <https://doi.org/10.1007/s40996-024-01396-8>
- [32] ASTM C618-03, "Standard specification for coal fly ash and raw or calcined natural pozzolan for use as a mineral admixture in concrete. United States: ASTM Standard, 2004.
- [33] ASTM C109, "Standard test method for compressive strength hydraulic cement mortars (Using 2-in. or [50-mm] Cube Specimens). United States: ASTM Standard, 2020.
- [34] D. L. Kong and J. G. Sanjayan, "Effect of elevated temperatures on geopolymer paste, mortar and concrete," *Cement and Concrete Research*, vol. 40, no. 2, pp. 334-339, 2010. <https://doi.org/10.1016/j.cemconres.2009.10.017>
- [35] A. A. Adam and X. Horiato, "The effect of temperature and duration of curing on the strength of fly ash based geopolymer mortar," *Procedia Engineering*, vol. 95, pp. 410-414, 2014. <https://doi.org/10.1016/j.proeng.2014.12.199>
- [36] K. Yomthong, D. Wattanasiriwech, P. Aungkavattana, and S. Wattanasiriwech, "Effect of NaOH concentration and curing regimes on compressive strength of fly ash-based geopolymer," *Materials Today: Proceedings*, vol. 43, pp. 2647-2654, 2021. <https://doi.org/10.1016/j.matpr.2020.04.630>
- [37] ASTM C642-97, "Standard test method for density, absorption, and voids in hardened concrete. United States: ASTM Standard, 2004.
- [38] ASTM C191-04, "Standard test method for time of setting of hydraulic cement by vicat needle. United States: ASTM Standard, 2004.
- [39] P. He *et al.*, "Effects of Si/Al ratio on the structure and properties of metakaolin based geopolymer," *Ceramics international*, vol. 42, no. 13, pp. 14416-14422, 2016. <https://doi.org/10.1016/j.ceramint.2016.06.033>

- [40] R. Wang, J. Wang, T. Dong, and G. Ouyang, "Structural and mechanical properties of geopolymers made of aluminosilicate powder with different SiO<sub>2</sub>/Al<sub>2</sub>O<sub>3</sub> ratio: Molecular dynamics simulation and microstructural experimental study," *Construction and Building Materials*, vol. 240, p. 117935, 2020. <https://doi.org/10.1016/j.conbuildmat.2019.117935>
- [41] P. S. Deb, P. Nath, and P. K. Sarker, "The effects of ground granulated blast-furnace slag blending with fly ash and activator content on the workability and strength properties of geopolymer concrete cured at ambient temperature," *Materials & Design (1980-2015)*, vol. 62, pp. 32-39, 2014. <https://doi.org/10.1016/j.matdes.2014.05.001>
- [42] R. C. Kaze *et al.*, "Microstructure and engineering properties of Fe<sub>2</sub>O<sub>3</sub> (FeO)-Al<sub>2</sub>O<sub>3</sub>-SiO<sub>2</sub> based geopolymer composites," *Journal of Cleaner Production*, vol. 199, pp. 849-859, 2018. <https://doi.org/10.1016/j.jclepro.2018.07.171>
- [43] J. Davidovits and R. Davidovits, "Ferro-Sialate Geopolymers (-Fe-O-Si-O-Al-O-)," *Geopolymer Institute Library*, pp. 1-6, 2020. <https://doi.org/10.13140/RG.2.2.25792.89608/2>
- [44] Y. Patrisia, D. W. Law, C. Gunasekara, and A. Wardhono, "Long-term durability of iron-rich geopolymer concrete in sulphate, acidic and peat environments," *Journal of Building Engineering*, vol. 97, p. 110744, 2024. <https://doi.org/10.1016/j.job.2024.110744>